Available online at www.sciencedirect.com
ScienceDirect
Journal of the European Ceramic Society 28 (2008) 2701–2708
www.elsevier.com/locate/jeurceramsoc

Pressureless brazing of zirconia to stainless steel with Ag–Cu filler metal and TiH_2 powder

G.W. Liu [a,*], G.J. Qiao [a,**], H.J. Wang [a], J.F. Yang [a], T.J. Lu [a,b]

[a] *State Key Laboratory for Mechanical Behavior of Materials, Xi'an Jiaotong University, Xianning West Road No. 28, Xi'an 710049, Shaanxi, China*
[b] *School of Aerospace, Xi'an Jiaotong University, , Xianning West Road No. 28, Xi'an 710049, Shaanxi, China*

Received 13 November 2007; received in revised form 6 April 2008; accepted 12 April 2008
Available online 27 May 2008

Abstract

Partially stabilized zirconia was joined to stainless steel by pressureless active brazing with Ag–Cu filler metal and TiH_2 powder. Microstructures, microchemistry and reaction products of the brazing seam were analyzed. The effects of brazing temperature and holding time on the joint shear strength were also investigated. The results showed that there existed three zones in the brazing seam and a double-layer structure at the ZrO_2/filler interface. Due to the difference in brazing condition, the microstructures including the thicknesses and compositions of the three zones and two layers were different. It is further found that Ti originated from TiH_2 coating diffused into the whole interlayer, resulting in the reaction products such as $CuTi_3$, Ti_3Cu_3O, Cu_4Ti_3, $NiTi_2$, Ni_3Ti and Ti. The maximum joint shear strength of over 90 MPa was obtained due to the improved interface bonding.

Keywords: Brazing; Microstructure; Interface; Strength; ZrO_2

1. Introduction

Zirconia is an important structural and functional material because of its high strength and fracture toughness, as well as good ionic conductor at elevated temperatures. For these reasons, zirconia can be applied in wire drawing dies, cutting and machining tools, oxygen sensors and hence fuel cells.[1] However, most of advanced ceramics, including zirconia are brittle and show a poor machinability, which makes it difficult to fabricate complex-shaped and large-sized components.[2,3] Joining of ceramic/metal can overcome these drawbacks to a great extent. The techniques for joining ceramics for high-temperature applications include sintering metal powder process, active metal brazing, and diffusion bonding, etc. Active metal brazing is an appropriate method for joining of zirconia ceramic in terms of structural reliability and economical industrialization. In particular, by the addition of Ti to some alloys this method can promote lower contact angles and hence wetting.[1] Over the past decades, many investigations on the joining of zirconia to metals or ceramics were obtained, with these alloys added with active Ti, such as Ag-base,[1–14] Cu-base[15–18] and Au-base brazes,[19,20] etc. Up to now, two methods are usually involved in the addition of Ti: smelting before brazing or fusing during brazing with these alloys. Most of previous studies used the former. However, the latter showed an advantage over the former for the Ti foil,[4] braze coating containing-TiH_2,[5] TiH_2 powder coating,[6] Ti vapor coatings,[13,14] and TiH powder coating.[16]

Usually mechanical load should be applied to improve brazing alloys spreading on the ceramic surface at brazing temperature, but this limits the application fields in industrial products with complicated shape. Pre-coating containing Ti on ZrO_2 surface can be used to solve this problem. TiH_2 coating was adopted to braze ZrO_2 to cupper,[6] but the strength was not investigated and microstructure was also not discussed in detail. In this paper, partially stabilized zirconia (PSZ) ceramic

* Corresponding author. Tel.: +86 29 82667942; fax: +86 29 82665443.
** Corresponding author. Tel: +86 29 82665221; fax: +86 29 82663453
E-mail addresses: lgwniat@yahoo.com.cn (G.W. Liu), gjqiao@mail.xjtu.edu.cn (G.J. Qiao), hjwang@mail.xjtu.edu.cn (H.J. Wang), yang155@mail.xjtu.edu.cn (J.F. Yang), TJLu@mail.xjtu.edu.cn (T.J. Lu).

0955-2219/$ – see front matter.
doi:10.1016/j.jeurceramsoc.2008.04.008

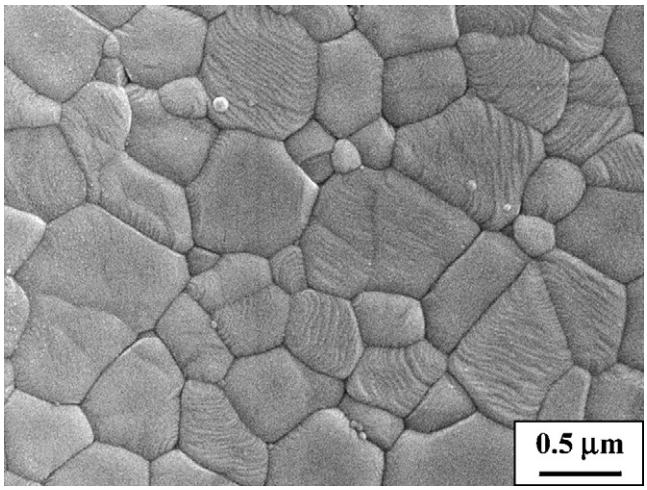

Fig. 1. Microstructure of the PSZ sample.

was brazed in vacuum to stainless steel at different brazing temperatures and holding times. The main aim of this work is to investigate the microstructure of zirconia/stainless steel joint fabricated by active brazing with Ag–Cu filler metal and TiH_2 powder, and to obtain high joint strength between two materials (zirconia ceramic and stainless steel) with significant difference in coefficient of thermal expansion (CTE) through pressureless joining technique.

2. Experimental procedure

2.1. Materials

ZrO_2–3 mol.% Y_2O_3 powder (average particle size ~0.3 μm, Shenzhen Nanbo Structure Ceramic Co., Ltd, Shenzhen, China) was used to prepare zirconia ceramic samples. The molding forming was adopted, with linear pressing up to 200 MPa for 30 s. The green bodies were sintered in air at 1550 °C for 2 h. PSZ ceramic pieces were obtained, with porosity, density and bending strength of 0.5%, 5.95 g/cm^3 and 850 MPa, respectively. Fig. 1 shows the microstructure of the polishing sample after thermal etching at 1400 °C × 60 min, which indicates average grain size of about 0.5–1 μm. The sizes of PSZ pieces used for brazing were Ø 17 mm × 6 mm. Common commercial stainless steel (AISI 304, S–S) was used as the metal component, with dimensions of Ø 10 mm × 5 mm. The average coefficient of thermal expansion (CTE, 0–600 °C) is about 10.0×10^{-6} °C^{-1} for PSZ[1] and 18.5×10^{-6} °C^{-1} for S–S.[21] The 72Ag–28Cu (wt.%) alloy filament was used as brazing solder with a diameter of Ø 0.8 mm. Commercial TiH_2 powder (Northwest Institute for Nonferrous Metal Research, Xi'an, China) was used, whose chemical composition is shown in Table 1. Before and after milling with roller for 80 h, the particle size distribution is shown in Fig. 2, and its meso-diameters D_{50} was 25.057 and 2.785 μm, respectively.

Table 1
The chemical composition of commercial TiH_2 powder (wt.%)

Ti	H	Fe	Cl	N	C	Si	Mg	Mn
96.72	3.45	0.06	0.06	0.04	0.03	0.02	0.01	0.01

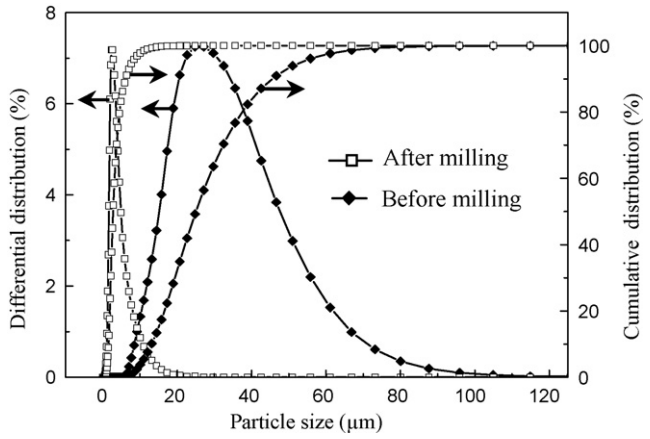

Fig. 2. Particle size distribution curves of TiH_2 powder after and before milling.

2.2. Joint sample preparation

The PSZ pieces, annular Ag–Cu alloy filaments and S–S columns were cleaned carefully. This procedure includes three steps: boiling in alkalescent scouring agent for 20 min, rinsing with distilled water and finally ultrasonic cleaning in acetone. The TiH_2 paste was prepared from a mixture of TiH_2 powder, diethyl oxalate and collodion in a ratio of 10 g:6 ml:8 ml. TiH_2 powder and diethyl oxalate were mixed firstly and then added with collodion. Ultrasonic vibrating and stirring were adopted to get a homogeneous mixture, named as TiH_2 paste. After the ceramic pieces were roasted for 80 °C × 3 h, one side of the PSZ piece surfaces was painted with the TiH_2 paste by writing brush and then air-dried. In order to promote the wettability of brazing alloy on S–S surface, a thin Ni layer was coated on the brazing surface of S–S columns by electro-plating in Watts' solution ($NiSO_4$ 280 g/L+ $NiCl_2$ 45 g/L + HBO_3 35 g/L + $C_{12}H_{25}SO_4Na$ 0.1 g/L) at a current density about 1 A/dm^2 for 30 min. PSZ pieces with TiH_2 coating, annular Ag–Cu alloy filaments and nickel-plated S–S columns were assembled as shown in Fig. 3, and finally brazed in a vacuum furnace (vacuity: 7×10^{-3} Pa, furnace model: High-multi 5000, Japan). At the first stage, the temperature of furnace was taken to 400 °C at a rate of 10 °C/min and maintained for 30 min. Subsequently, the temperature was raised to 750 °C at 6 °C/min and kept for 10 min. Then the temperature was taken to the brazing temperature (820–860 °C) at the speed of 5 °C/min and held for 10–50 min followed by gradual cooling at a speed less than 10 °C/min. The flow chart for the preparation process of PSZ/S–S joints is shown in Fig. 4.

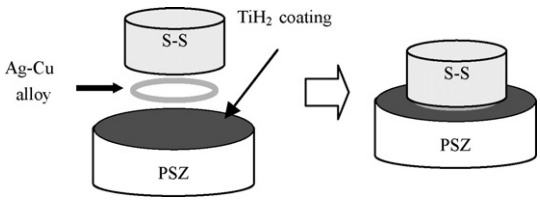

Fig. 3. Chart of assembling the brazing parts.

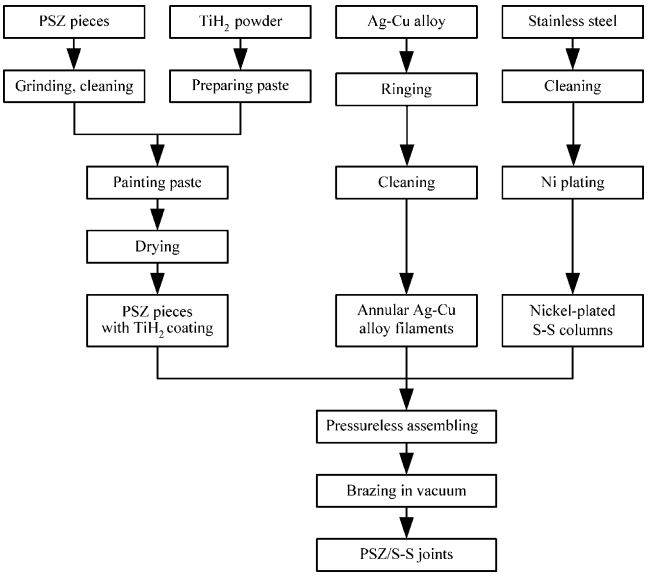

Fig. 4. Flow chart for the preparation process of PSZ/S–S joints.

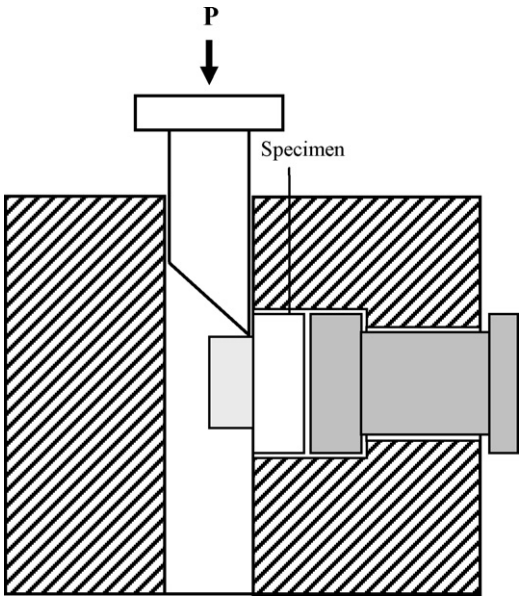

Fig. 5. The clamp and assemble chart for shear strength testing.

2.3. Sample characterization

Some PSZ/S–S joints were cut off along the direction vertical to the joint line and polished. Theirs microstructures of joint were characterized by scanning electron microscopy (SEM, Model Quanta-2000, Philips-PET, Ltd., Holland, or JSM-7000F, JEOL, Japan). Energy dispersive spectroscopy (EDS, Model Oxford INCA, British) was also adopted to determine element composition of the microstructural characteristic and their distribution in the brazing seam. The phase compositions and reaction products in the brazing area were identified by X-ray diffraction (XRD, Model X'Pert PRO, PANalytical, Ltd., Holland) analysis at 40 kV and 40 mA using Cu Kα radiation.

The joint strength was tested by shear-load method using an Instron-1195 testing machine. A special clamp was adopted, as shown in Fig. 5. The loading speed was 0.5 mm/min. The mean value of joint strength under each brazing condition was the arithmetical average of five joint samples.

3. Results and discussion

3.1. Microstructure

The SEM images of the PSZ/S–S joint cross section at 850 °C × 30 min are shown in Fig. 6. Three main zones (I, II and III) with distinguished microstructure difference crossing the brazing interlayer were formed. Fine microstructure adjacent to ceramic side appeared for the zone I, whose thickness was equivalent to that of the original TiH_2 coating. Zone III near S–S side also had fine microstructure and equivalent thickness of the Ni plating layer. Zone II in the middle had obviously coarser microstructure than that of zones I and III, which was related to the crystallization of compounds and the fewer nucleation cores. The white blocks in the three zones were Ag-rich phases, according to EDS analysis, and the black ones included Ti, Cu and Ni. At the heating stage, the organics (diethyl oxalate and collodion) in TiH_2 coating were evaporated firstly, and then TiH_2 was decomposed to form a loose Ti layer on PSZ surface. Compared with Ti-containing alloys filler method, this neonatal Ti in situ decomposed from TiH_2 had fine particle size and clean surface, leading to higher reaction activity. When the eutectic temperature was reached, Ag–Cu alloy started to melt and penetrated into the loose Ti layer, and reactions of Ti/ZrO_2 and Ti/Ag–Cu alloy occurred simultaneously, forming the zone I. At the same time, the neonatal Ti and the Ni (mainly originated from the Ni coating on S–S surface) diffused into the Ag–Cu molten layer from both sides. Reacting, dissolving and precipitating processes took place continuously. Finally, in the middle (zone II) there appeared big white and black blocks. It is also shown from Fig. 6(c) that the zone III mainly consisted of Ag-rich solid solution, which presented as a bright belt. It is fantastic that the original Ni coating disappeared due to its diffusing or dissolving into the molten alloy (also see Section 3.2).

For the ceramic/metal brazing, usually the microstructure of thin layers near ceramic surface affects joint properties remarkably. Double-layer structure was found between ZrO_2 and zone I, as shown in Fig. 6(d). As the Ti/ZrO_2 reaction layer, a black band near ZrO_2 ceramic matrix was composed of Zr, O and Ti from EDS analysis. A gray layer containing Ti, O, Cu and minor Zr was closed to the reaction layer, which was named as (Ti, O, Cu) sublayer here. The two thin layers presented similar thickness (∼1 μm) and legible interface, which are important for strong bonding.

The cross section of PSZ/S–S joint brazed at 830 °C × 20 min is shown in Fig. 7(a). Compared the Fig. 6(a) with Fig. 7(a), it can be seen that, although the two brazing conditions (830 °C × 20 min and 850 °C × 30 min) gave similar microstructure with three zones and two interfacial layers, some obvious differences were also found. At lower brazing temperature or shorter holding time (Fig. 7(a)), zone II presented finer structure (smaller phase blocks) and much more white phases

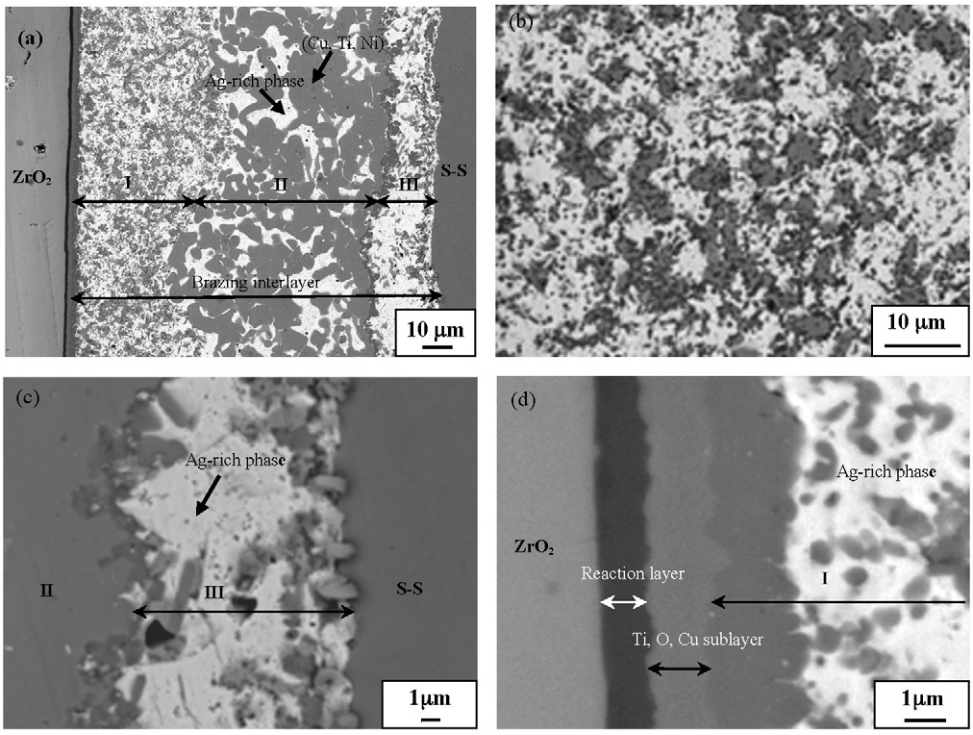

Fig. 6. SEM images of the joint cross section at 850 °C × 30 min: (a) whole brazing seam; (b) zone I; (c) near stainless steel; (d) PSZ/filler interface.

(Ag-rich phases). Zone III brazed at 850 °C × 30 min appeared as a wide bright belt and no Ni coating layer was found, while Ni coating layer brazed at 830 °C × 20 min was retained. With brazing temperature increasing, Ti and Ni have higher activity and solubility in Ag–Cu alloy, resulting in much more black phases in the zone II and disappearance of Ni-coating. Higher brazing temperature and longer holding time increased the thickness of reaction layer, as shown in Figs. 6(d) and 7(b), which was related to the high strength of 850 °C × 30 min samples (Fig. 11).

3.2. Microchemistry

The seven elements of interest, Ag, Cu, Ti, Ni, Zr, O and Fe, originated from the ZrO_2 ceramic matrix, stainless steel, Ag–Cu filler metal, TiH_2 and Ni coatings. In order to determine the element distribution and migration behavior, EDS analysis was adopted by line-scanning type for these elements to the sample at 850 °C × 30 min. Fig. 8 shows the elemental EDS profiles across the whole brazing area. The white line in the top picture was scanning line. The bright continuous block corresponded to Ag profile, indicating that Ag existed in all the three zones as Ag-rich phase marked in Fig. 6. Similar to Ag, Cu and Ti were also found in all the three zones. Although Cu was detected in the Ag-rich phase, it mainly existed in the dark phase. The element distribution profile of Ti was similar to that of Cu, except in zone III. A little Cu (∼10 wt.%) was detected in the bright blocks, but no Ti was found, which could explain the slight difference between Ti and Cu profiles. Even in zone III near S–S surface, Ti can be detected, indicating that Ti migrated for a long distance due to its high activity and solubility in filler metal at the brazing temperature. Zr only existed in ZrO_2 ceramic matrix and reaction layer near the ZrO_2 surface. Oxygen mainly existed in the two sides of brazing area, which originated from ZrO_2 ceramic matrix and oxygen in the S–S. Further EDS analysis revealed that some oxygen from ZrO_2 migrated into the middle position of zone I. It is noted that, compared with metal elements, the oxygen content by EDS analysis is not very precise. So the element distribution profile of oxygen was only a reference. Ni and Fe presented unusual element distribution profiles, as shown in Fig. 8. Both of them derived from metal side, i.e. stainless steel or Ni coating, and their contents were very low in zone III near S–S surface. Ni mainly existed in zone II, and its profile corresponded to that of Ti, indicating that Ni and Ti coexisted in the same phase (dark blocks in zone II). Fe was detected with abnormal content at zone II/III boundary. Cu and Ti had a strong mutual affinity and coexisted as intermetallics in zones I and II, and Ag was abundant in zone III. Furthermore, little Ni and Fe could appear in zone III due to their low solid solubility in Ag, however, a series of compounds can be formed due to high solid solubility between the two of the three elements (Ni, Cu and Ti). Therefore, Ni mainly existed in zone II. However, due to the higher melting point of Fe and low solid solubility in both Cu and Ag at room temperature, it was difficult for Fe to diffuse a long distance.

Fig. 9 shows the elemental EDS profiles across the ceramic/filler interface, indicating that the reaction layer contained Ti, O and Zr. The sublayer was composed of Ti, O, Cu and minor Zr. It is noteworthy that Ag was hardly detected in the two layers. The reaction layer was produced by chemical reaction between the ZrO_2 matrix and active Ti (decomposed from TiH_2 coating), which was different from formation of

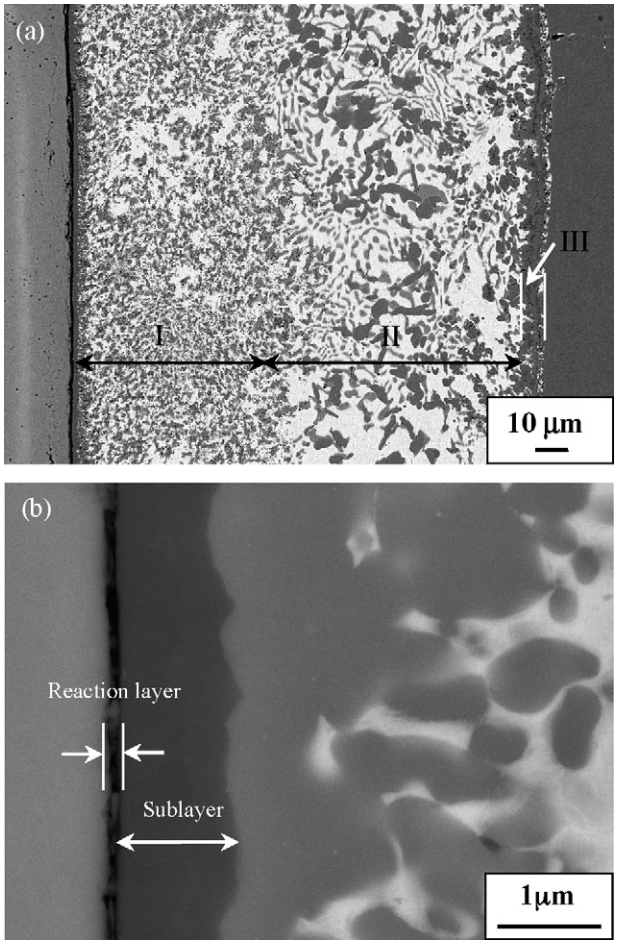

Fig. 7. SEM images of the joint cross section at 830 °C × 20 min: (a) whole brazing seam; (b) PSZ/filler interface.

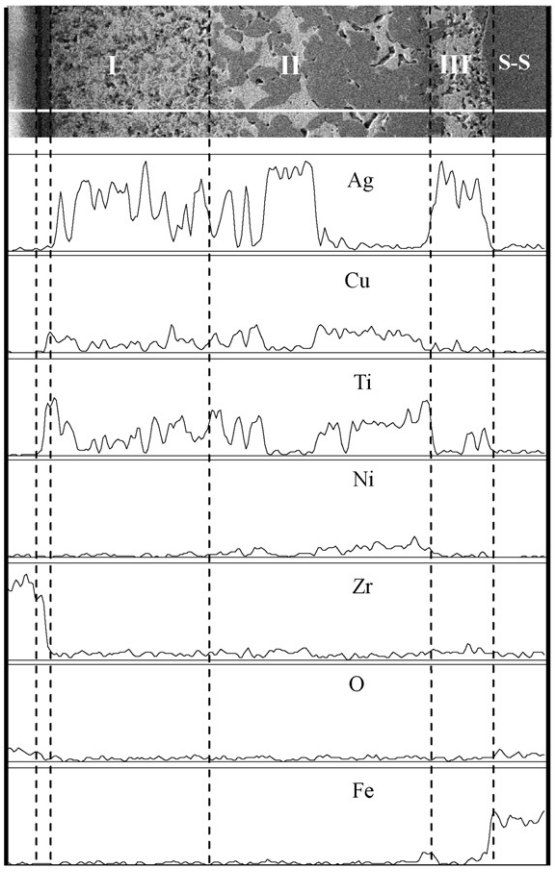

Fig. 8. Elemental EDS profiles across the whole brazing area.

zones I, II and III. The sublayer mainly derived from chemical reaction among Ti, Cu and O, in which there were strong interactions. Therefore, the two layers existed as a dense double-layer structure, and it was very difficult for Ag to migrate into these layers.

3.3. Phase composition

In order to determine the existing forms of Ti in the brazing seam, a shear broken sample at 850 °C × 30 min that fractured along the reaction layer was analyzed by means of XRD, which was thinned layer-by-layer by polishing along the parallel surface to the brazing interlayer. Fig. 10 shows XRD patterns of the corresponding layer positions.

From Fig. 10, the Ag element existed in the three zones as pure silver or Ag-rich solid solution, but the Cu did in the forms of compound. The products containing Ti were found in the whole brazing area, whose existing forms were greatly different. Ti usually existed in compounds due to its high activity, however, elemental Ti was found in zone III, as shown in the curves (f) and (g), due to low solid solubility of Ti in Ag or Ag-rich solution. Ni-containing phases mainly existed in the zone II rather than zone III, as $NiTi_2$ and Ni_3Ti intermetallics instead of alloy,

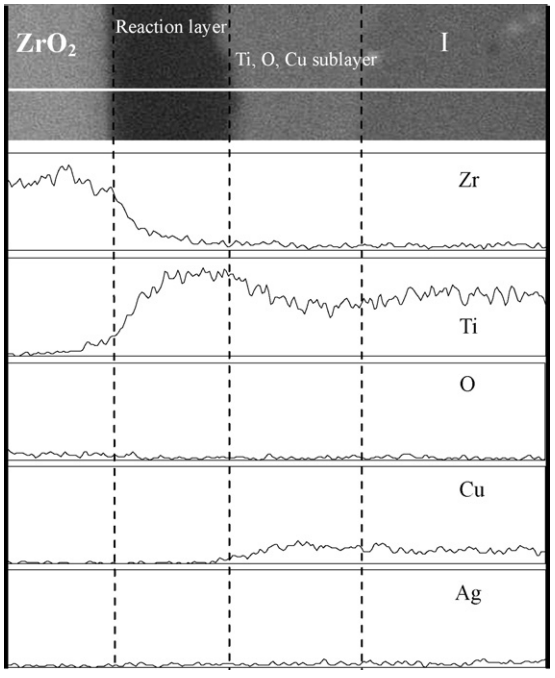

Fig. 9. Elemental EDS profiles across the ceramic/filler interface.

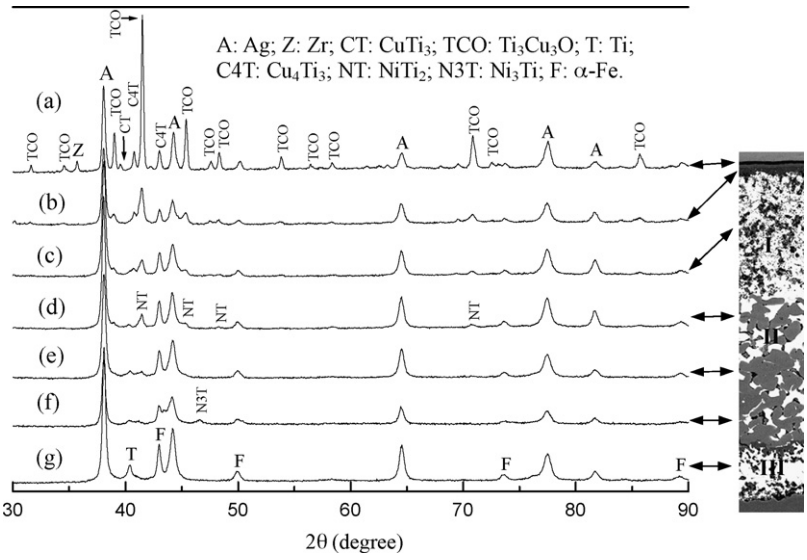

Fig. 10. XRD patterns of the corresponding layer positions: (a) reaction layer; (b and c) zone I; (d–f) zone II; (g) zone III.

although most of Ni originated from the Ni coating on the S–S surface. A reasonable explanation was that the diffusion of Ni for a long distance into zone II was brought on by the high active Ti, resulting in reactions between them. The XRD and EDS (in Fig. 8) results for Ti and Ni had good consistency. Furthermore, by comparing curves (a), (b) and (c), one can see that $CuTi_3$ and Zr mainly coexisted in the neighbor of the (Ti, Cu, O) sublayer, and the Ti_3Cu_3O phase mainly existed in the zone I near the interface, indicating that the oxygen diffused from ZrO_2 side to a limited distance of about 30 μm. In addition, the Cu_4Ti_3 phase mainly existed in zones I and II. So in the brazing area, from ceramic side to metal side, the evolution of Ti-containing products was $CuTi_3$, Ti_3Cu_3O, Cu_4Ti_3, $NiTi_2$, Ni_3Ti and Ti in turn.

3.4. Mechanical properties

Fracture strength and reliability of ceramic/metal joint are of a great importance. The main factors affecting joint mechanical properties are involved in joining process and characters of the joined materials (ceramic and metal). The effects of brazing temperature and holding time on joint shear strength are shown in Fig. 11. From Fig. 11, brazing temperature gave a more remarkable influence on joint strength than the holding time. In the ranges of brazing temperature and holding time, the joint strength increased firstly. The maximum shear strength was over 90 MPa, and the average strength was about 75 MPa at 850 °C × 30 min. With brazing temperature increasing or holding time extending, the neonatal active Ti originated from TiH_2 would react with ZrO_2 ceramic and filler metal more fully, therefore a firm reaction layer with a good bonding was formed, just as showed in Fig. 6. Contrarily, when the temperature was too high or holding time was too long, the neonatal active Ti reacted excessively with the ceramic and the alloy. As a result, more brittle intermetallics were formed near the interface and in the brazing interlayer, and hence the interface was weakened. Furthermore, the residual stress in the joint was accumulated with those brittle products thickening. Both the weakened interface and large residual stress led to a lower joint strength, when the temperature was raised over 850 °C or the holding time was prolonged over 30 min.

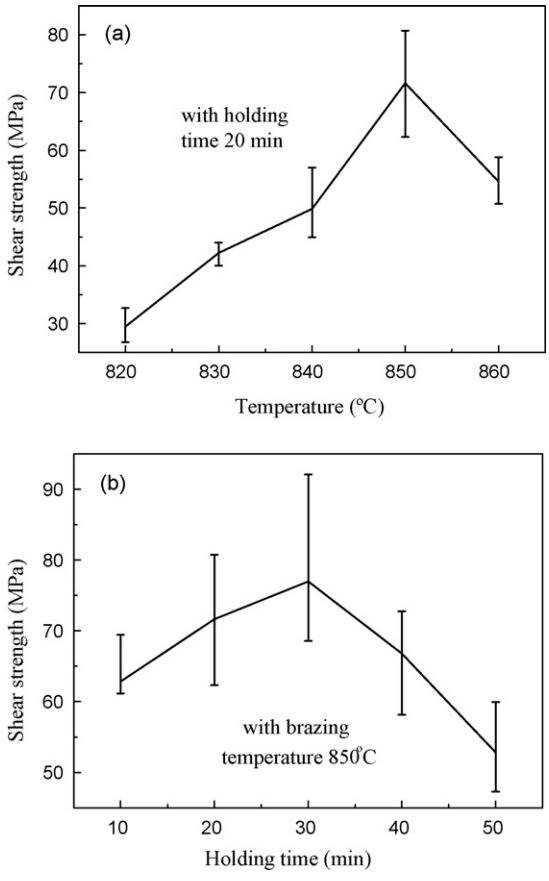

Fig. 11. Joint shear strength at different conditions: (a) brazing temperatures and (b) holding times.

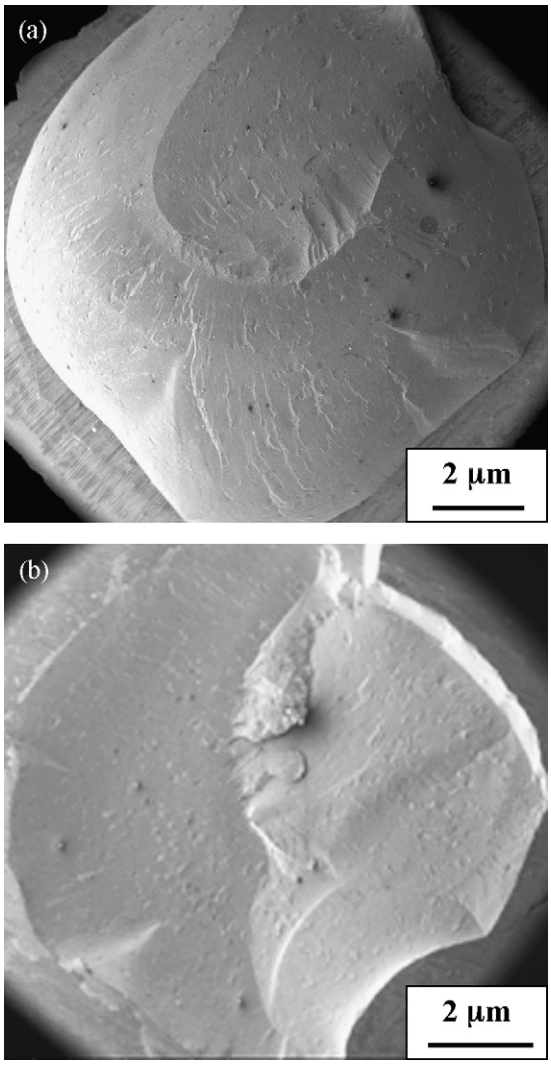

Fig. 12. Shear broken joints fractured in the ceramic matrix: (a) metal side; (b) ceramic side.

Most of the joint fractures developed in the ceramic matrix near the ceramic/filler interface, as shown in Fig. 12, because the maximum residual stress in ceramic matrix appeared at the position under the interface to a certain distance related to joint sizes. Only several samples fractured along the reaction layer and gave lower strength. The lower the temperature or the shorter holding time was, the higher the possibility of joint fracture along reaction layer was.

4. Conclusions

Zirconia ceramic was joined to stainless steel by pressureless active brazing with Ag–Cu filler metal and TiH_2 powder. Microstructures, microchemistry and reaction products of the brazing seam were analyzed. The effects of brazing conditions on the joint shear strength were investigated.

Three zones with microstructural difference in the brazing seam and a double-layer structure including a reaction layer and a sublayer at the ZrO_2/filler interface were formed. Due to the difference of brazing condition, the microstructures including the compositions of the three zones and the thicknesses of two layers were different. From ceramic side to metal side, the evolution of Ti-containing products in the brazing seam was from $CuTi_3$, Ti_3Cu_3O, Cu_4Ti_3, $NiTi_2$, Ni_3Ti and Ti in turn. In the ranges of brazing temperature and holding time, the joint strength increased firstly and the maximum strength of about 90 MPa, and the average strength over 75 MPa were attained at the optimum brazing condition. Brazing temperature gave a more remarkable influence on joint strength than the holding time.

Acknowledgements

This work was supported by the National Fundamental Research Program of China (Grant no. 2006CB601200).

References

1. Hanson, W. B., Ironside, K. I. and Fernie, J. A., Active metal brazing to zirconia. *Acta Mater.*, 2000, **48**, 4673–4676.
2. Hao, H., Wang, Y., Jin, Z. and Wang, X., Joining of zirconia ceramic to stainless steel and itself using $Ag_{37}Cu_{38}Ti_5$ filler metal. *J. Am. Ceram. Soc.*, 1995, **78**, 2157–2160.
3. Hao, H. Q., Wang, Y. L., Jin, Z. H. and Wang, X. T., Joining zirconia to zirconia using Ag–Cu–Ti filler metal. *J. Mater. Process. Technol.*, 1995, **52**, 238–247.
4. Wang, L. D., Wang, Y. H., Li, W. Z., Li, H. D. and Oki, T., Reaction behavior of ZrO_2/Ti interface in joining zirconia ceramics and stainless steel 304 with Ti foil. *Acta Metall. Sin.*, 1997, **33**, 756–762.
5. Kim, J. Y., Hardy, J. S. and Weil, K. S., Silver-copper oxide based reactive air braze for joining yttria-stabilized zirconia. *J. Mater. Res.*, 2005, **20**, 636–643.
6. Wu, Y. Q., Gao, L. Q. and Hu, M. H., The interfacial structure and mechanism of ZrO_2 ceramic to copper joining. *Vacuum Electron.*, 1995, **4**, 1–7.
7. Chuang, T. H., Yeh, M. S. and Chai, Y. H., Brazing of zirconia with AgCuTi and SnAgTi active filler metals. *Metall. Mater. Trans. A*, 2000, **31A**, 1591–1597.
8. Sciti, D., Bellosi, A. and Esposito, L., Bonding of zirconia to super alloy with the active brazing technique. *J. Eur. Ceram. Soc.*, 2001, **21**, 45–52.
9. Muolo, M. L., Ferrera, E., Morbelli, L. and Passerone, A., Wetting, spreading and joining in the alumina–zirconia–Inconel 738 system. *Scripta Mater.*, 2004, **50**, 325–330.
10. Smorygo, O., Kim, J. S., Kim, M. D. and Eom, T. G., Evolution of the interlayer microstructure and the facture modes of the zirconia/Cu–Ag–Ti filler/Ti active brazing joints. *Mater. Lett.*, 2007, **61**, 613–616.
11. Wang, X.-L., Hubbard, C. R., Spooner, S., David, S. A., Rabin, B. H. and Williamson, R. L., Mapping of the residual stress distribution in a brazed zirconia-iron joint. *Mater. Sci. Eng. A*, 1996, **211**, 45–53.
12. Xue, X. M., Wang, J. T. and Sui, Z. T., Wettability and interfacial reaction of alumina and zirconia by reaction silver–indium base alloy at mid-temperatures. *J. Mater. Sci.*, 1993, **28**, 1317–1322.
13. Hammond, J. P., David, S. A. and Santella, M. L., Brazing ceramic oxides to metals at low temperatures. *Weld. J.*, 1988, **67**, 227-s–232-s.
14. Santella, M. L. and Pak, J. J., Brazing titanium-vapor-coated zirconia. *Weld. J.*, 1993, **72**, 165s–172s.
15. Moorhead, A. J. and Keating, H., Direct brazing of ceramics for advanced heavy-duty diesels. *Weld. J.*, 1986, **65**, 17–30.
16. Durov, A. V., Kostjuk, B. D., Shevchenko, A. V. and Naidich, Y. V., Joining of zirconia to metal with Cu–Ga–Ti and Cu–Sn–Pb–Ti fillers. *Mater. Sci. Eng. A*, 2000, **290**, 186–189.
17. Durov, A. V., Naidich, Y. V. and Kostyuk, B. D., Investigation of interaction of metal melts and zirconia. *J. Mater. Sci.*, 2005, **40**, 2173–2178.

18. Petzow, G., Suga, T., Elssner, G. and Dvorak, U., Bond strength of vacuum brazed Mg-PSZ/steel joints. *Mater. Res. Bull.*, 1987, **22**, 1187–1193.
19. Singh, M., Shpargel, T. P. and Asthana, R., Brazing of stainless steel to yttria-stabilized zirconia using gold-based brazes for solid oxide fuel cell applications. *Int. J. Appl. Ceram. Technol.*, 2007, **4**, 119–133.
20. Agathopoulos, S., Correia, R. N., Joanni, E. and Fernandes, J. R. A., Interactions at zirconia-Au-Ti interfaces at high temperatures. Euro Ceramics VII. *Key Eng. Mater.*, 2002, **206-2**(pt 1–3), 487–490.
21. Li, C. S. and Huang, D. B., *Handbook of Materials for Mechanical Engineering*. Electronic Industry Press, Beijing, 2006, p. 453.